Anomalous charge pumping in a one-dimensional optical superlattice

Ran Wei and Erich J. Mueller
Laboratory of Atomic and Solid State Physics, Cornell University, Ithaca, New York 14853, USA
(Received 13 February 2015; published 7 July 2015)

We model atomic motion in a sliding superlattice potential to explore "topological charge pumping" and to find optimal parameters for experimental observation of this phenomenon. We analytically study the band structure, finding how the Wannier states evolve as two sinusoidal lattices are moved relative to one another, and relate this evolution to the center-of-mass motion of an atomic cloud. We pay particular attention to counterintuitive or anomalous regimes, such as when the atomic motion is opposite to that of the lattice. We propose a practical cold-atom experiment to detect this anomalous behavior. Through numerical simulations, we find that a *negative* adiabatic current and a nontrivial Chern number $\mathcal{C} = -1$ are readily measured.

DOI: 10.1103/PhysRevA.92.013609 PACS number(s): 67.85.Lm, 03.65.Vf

I. INTRODUCTION

Slow periodic changes in a lattice potential can transport charge. For a filled band, the integrated particle current per cycle in such an adiabatic pump is quantized [1]. We study a simple but rich example of this phenomenon, namely charge transport in a sliding superlattice, and draw attention to its counterintuitive properties such as regimes where the charge moves faster than the potential or even travels in the opposite direction. The mathematics predicting this anomalous transport goes back 30 years [2,3], but has not been observed in experiments. Here we argue that this effect is observable in a cold-atom experiment.

The quantum mechanics of particles in a one-dimensional (1D) superlattice is rich, for incommensurate periods boasting a fractal energy spectrum [4] and a localization transition similar to what is seen in disordered lattices [5]. While recent studies have focused on the tight-binding limit (the Aubry-Andre model) [6–23], we study the continuous limit of the 1D superlattice where, because of the weak potential, the single-particle spectra can be calculated perturbatively. Related cold-atom proposals on quantized transport [24–29] have focused on the simplest superlattice where one sublattice constant is half of the other, and the lowest band is therefore not in the anomalous regime which interests us. Reference [24] draws attention to the anomalous retrograde motion of particles in the second band, an approach which complements our ground-state proposal.

The 1D superlattice can be mapped onto the Harper-Hofstadter model [4,30]. The topological numbers (Chern numbers) associated with charge pumping can be mapped onto quantized Hall conductances [2,31]. Recent experiments involving artificial gauge fields on a 2D optical lattice have aimed to measure these 2D Chern numbers [32–36]. There are also related studies based on measurement of Hall drift [37], Bloch oscillations [38,39], Zak phase [40–42], time-of-flight images [43–45], edge states [46–51], or density plateaus [52,53].

In this paper, we study the charge transport in a 1D sliding superlattice, where the moving lattice period is an arbitrary rational multiple of the static lattice. We analytically calculate energy-band gaps and the topological invariants which give the integrated adiabatic current per pumping cycle [1]. The fact that this current can be made *arbitrarily large* and/or *opposite* to the direction of the sliding potential is counterintuitive. We present a physical interpretation of this phenomenon in terms of the quantum tunneling of Wannier functions between minima in the potential. We propose an experiment to detect this anomalous adiabatic current, and derive the optimal parameters. Through numerical simulations, we confirm that a *negative* integrated current and a nontrivial Chern number $\mathcal{C} = -1$ are readily measured in an experiment. We analyze corrections to adiabaticity, the harmonic trap, multiband effects, and finite-size effects.

II. MODEL

We consider the Hamiltonian of a 1D superlattice where one lattice adiabatically slides relative to the other,

$$H = \int dx\, \psi^\dagger(x)\left[-\frac{\hbar^2}{2m}\partial_x^2 + V_1(x,\varphi) + V_2(x)\right]\psi(x), \quad (1)$$

where $\psi(x)$ represents the field operator of the particle, $\hbar$ is Planck's constant, and m is the mass of the particle. The periodic potentials $V_1(x,\varphi) = 2v_1\cos(px-\varphi)$ and $V_2(x) = 2v_2\cos(qx)$ are commensurate, with lattice constants $2\pi/p$ and $2\pi/q$, and intensities v_1 and v_2. We take the relative phase φ to be slowly varying in time. The period of the Hamiltonian is set by the greatest common divisor of p and q, i.e., $\kappa \equiv \gcd(p,q)$, as illustrated in the inset of Fig. 1. Treating $1/\kappa$ as the unit length, we redefine $x\kappa \to x$, $p/\kappa \to p$, and $q/\kappa \to q$. Treating $E_r = \hbar^2\kappa^2/m$ as the unit energy, we redefine $H/E_r \to H$, $v_1/E_r \to v_1$, and $v_2/E_r \to v_2$. The dimensionless Hamiltonian in the momentum space is then

$$H = \sum_k \frac{k^2}{2}\psi_k^\dagger\psi_k + \left(v_1 e^{-i\varphi}\psi_k^\dagger\psi_{k+p} + v_2\psi_k^\dagger\psi_{k+q} + \text{H.c.}\right). \quad (2)$$

Here, $\psi_k = \frac{1}{\sqrt{L}}\int dx\, e^{ikx}\psi(x)$, with dimensionless system length L and dimensionless momentum k. Since states of momentum k are coupled only to those of momentum $k+n$ for integer n, we restrict ourselves to the first Brillouin zone ($0 \leqslant k < 1$) and rewrite the Hamiltonian,

$$H = \sum_{0\leqslant k<1}\sum_{n=-\infty}^{\infty}\frac{1}{2}(k+n)^2\psi_n^\dagger\psi_n + \left(v_1 e^{-i\varphi}\psi_n^\dagger\psi_{n+p} + v_2\psi_n^\dagger\psi_{n+q} + \text{H.c.}\right), \quad (3)$$

where we have suppressed the k index, writing $\psi_n \equiv \psi_{k+n}$.

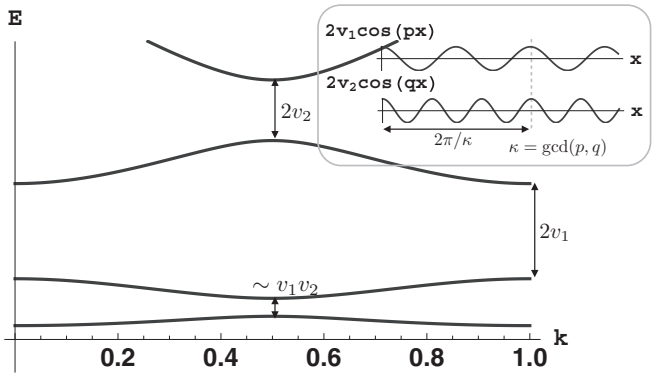

FIG. 1. Band structure of a 1D superlattice for $p = 2, q = 3$, showing energy E vs dimensionless wave vector k for weak potentials. Inset: The two potentials making up the superlattice and the unit cell with period set by the greatest common divisor $\kappa \equiv \gcd(p,q)$. For this choice of p and q, the energy gap between the third and fourth band is set by the potential strength $2v_2$, the gap between the second and third band is set by the potential strength $2v_1$, and the small gap is set between the second and third band scales as $\sim v_1 v_2$.

To illustrate the resulting band structure, we impose a cutoff on n and numerically diagonalize the Hamiltonian in Eq. (3) for $p = 2$ and $q = 3$. The lowest four energy bands are shown in Fig. 1, and even for this simple case, the gaps display a range of behaviors for small v_1 and v_2. The gap between the third and fourth band is induced by the potential $V_2(x)$ and is proportional to v_2 for weak potentials. The gap between the second and third band is induced by $V_1(x)$ and is proportional to v_1. The small gap between the second and third band is induced by the combination of these two potentials, which scales as $\sim v_1 v_2$. In the following section, we will discuss the origin of these scalings in the context of understanding the lowest-energy gap.

III. BAND GAPS AND TOPOLOGY

The eigenstates of the Hamiltonian in Eq. (3) can be found perturbatively in the limit of $v_1, v_2 \ll 1$. Suppressing the index k, we write $H = H_0 + \lambda H_1$, with

$$H_0 = \sum_{n=-\infty}^{\infty} \frac{1}{2}(k+n)^2 \psi_n^\dagger \psi_n, \tag{4}$$

$$\lambda H_1 = \lambda_p H_p + \lambda_{-p} H_{-p} + \lambda_q H_q + \lambda_{-q} H_{-q}, \tag{5}$$

where $H_p = \sum_{n=-\infty}^{\infty} \psi_n^\dagger \psi_{n+p}$, $H_q = \sum_{n=-\infty}^{\infty} \psi_n^\dagger \psi_{n+q}$, and λ is a formal small parameter, with $\lambda_p = \lambda_{-p}^* = v_1 e^{-i\varphi}$ and $\lambda_q = \lambda_{-q}^* = v_2$.

For small λ and $0 \leqslant k < 1$, the eigenstates of the lowest band will be superpositions of $|-1\rangle$ and $|0\rangle$, where $|m\rangle = \psi_m^\dagger |\text{vac}\rangle$. We let $\delta k = k - 1/2$ denote the distance of k from the band crossing point and assume $\delta k > 0$. The physics for $\delta k < 0$ is analogous. While ordinary perturbation theory works far from the crossing ($\delta k \gg \epsilon$, where ϵ will be precisely defined below), one must use higher-order degenerate perturbation theory to find the eigenstates for $\delta k \lesssim \epsilon$. As argued in the Appendix, the resulting effective Hamiltonian is of the form

$$H_{\text{eff}} = P H_0 P + \sum_{\substack{s_+, s_- \geqslant 0 \\ r_+, r_- \geqslant 0}} \lambda_p^{s_+} \lambda_{-p}^{s_-} \lambda_q^{r_+} \lambda_{-q}^{r_-} \mathcal{L}^{(s_+, s_-, r_+, r_-)}, \tag{6}$$

where $P = |-1\rangle\langle -1| + |0\rangle\langle 0|$, and s_+, s_-, r_+, r_- are integers. The operator $\mathcal{L}^{(s_+, s_-, r_+, r_-)}$ is the contribution to H_{eff} involving the absorption of $\eta = sp + rq$ units of momentum from the lattices, where $s = s_+ - s_-$ and $r = r_+ - r_-$. By conservation of momentum, $\alpha \equiv \langle -1 | \mathcal{L}^{(s_+, s_-, r_+, r_-)} | 0 \rangle = 0$ unless $\eta = 1$. We linearize H_{eff} about $\delta k = 0$, and write the operators in the basis $\{|-1\rangle, |0\rangle\}$. At the lowest nontrivial order, we have

$$\mathcal{H}_{\text{eff}} = \begin{pmatrix} -\frac{1}{2}\delta k & \alpha \Delta e^{i\chi} \\ \alpha \Delta e^{-i\chi} & \frac{1}{2}\delta k \end{pmatrix} + \text{const}, \tag{7}$$

where $\Delta = v_1^{|r_m|} v_2^{|s_m|}$, $\chi = -s_m \varphi$, and s_m, r_m correspond to the absolutely smallest solution to the Diophantine equation $sp + rq = 1$. This result agrees with a similar perturbative analysis carried out by Thouless *et al.* [2] and Niu [3] for related models.

The off-diagonal terms of Eq. (7) split the energy degeneracy at $\delta k = 0$ and create an energy gap of size $\Delta E_g \equiv 2|\alpha \Delta|$. For example, if $p = 2, q = 3$, the absolutely smallest solution to the Diophantine equation has $s_m = -1$, $r_m = 1$, as $-p + q = 1$. Thus the energy gap is $2|\alpha v_1 v_2|$, as denoted in Fig. 1. For larger $|s_m|$ and $|r_m|$, the energy gap can be extremely small. Ordinary perturbation theory would have sufficed in the regime where $\delta k \gg 2|\alpha \Delta|$, allowing us to identify ϵ as $2|\alpha \Delta|$. Properties of higher bands can be analyzed similarly.

By analyzing Eq. (7), we find that the lowest-energy eigenstate of Eqs. (4) and (5) has the form

$$|k, \varphi\rangle = -\sin\frac{\beta}{2} e^{i\chi/2} |-1\rangle + \cos\frac{\beta}{2} e^{-i\chi/2} |0\rangle + \cdots, \tag{8}$$

where $\tan\beta = -2\alpha\Delta/\delta k$. The neglected terms are higher order in v_1 and v_2. For $\delta k \gg 2|\alpha\Delta|$, $\sin\frac{\beta}{2} \approx 1$ and $\cos\frac{\beta}{2} \approx 0$, and the coefficients are featureless.

Slowly changing φ generates an adiabatic current [1]. For a completely filled band, the integrated current in one pumping period (φ from 0 to 2π) is [54]

$$\Delta Q = 2\pi \mathcal{C} = \int_0^1 dk \int_0^{2\pi} d\varphi \, \Omega_{k\varphi}, \tag{9}$$

where the Berry curvature is

$$\Omega_{k\varphi} = i(\partial_\varphi \langle k, \varphi | \partial_k | k, \varphi \rangle - \text{H.c.}) = \frac{s_m}{2} \partial_k \cos\beta. \tag{10}$$

We see $\Omega_{k\varphi}$ is concentrated near the location of the energy gap. Integrating the Berry curvature is trivial, yielding the Chern number $\mathcal{C} = s_m$. Although our argument requires that v_1 and v_2 are small, due to the quantized nature of $\mathcal{C}$, the result should hold for all nonzero v_1 and v_2. In our numerical calculations with larger v_1, v_2, we find the curvature is roughly uniform over the Brillouin zone, but as expected its integral is unchanged.

IV. ANOMALOUS CHARGE PUMPING

By appropriately choosing p and q, one can make $\mathcal{C} = s_m$ an arbitrary integer [3,55–58]. This means that in one pumping cycle, a single particle may move arbitrarily far and/or opposite to the direction of the sliding potential. Such

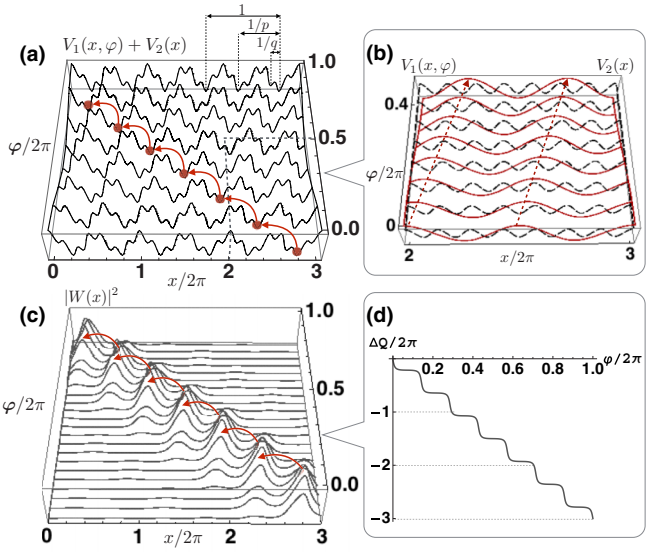

FIG. 2. (Color online) (a) Illustration of adiabatic charge transport in a 1D superlattice, where the particle "travels" through three unit cells to the left when the lattice potential moves to the right by one period. Solid lines show the potential $V_1(x,\varphi)+V_2(x)$ for different values of φ. Arrows schematically show how the locations of the minima shift discontinuously. (b) Illustration of the evolution of two separated potentials of the superlattice: the right-sliding potential $V_1(x,\varphi)$ (solid red) and the static potential $V_2(x)$ (dashed black). (c) Evolution of the Wannier function. Arrows indicate the "tunneling" process. (d) The evolution of integrated adiabatic current as a function of φ. In these plots, we choose $p=2$ and $q=7$, so the Chern number is $\mathcal{C}=s_m=-3$. Other parameters are $v_1=0.5$ and $v_2=0.25$.

long-distance and/or retrograde transport seems unphysical. The magic comes from the adiabatic process: If the potential moves sufficiently slowly, the particles always stay in a global minimum of the potential. Due to the structure of the superlattice, a slight motion of the potential could result in a dramatic change of the locations of the global minima [see Fig. 2(a)]. Within a small portion of a pumping cycle, the particles may "tunnel" to the new global minima which could be a large distance away from the old minima.

To further quantify our interpretations, we calculate the integrated current

$$\Delta Q(\varphi)=\frac{1}{2\pi}\int_0^1 dk\int_0^{\varphi}d\varphi'\,\Omega_{k\varphi'}, \tag{11}$$

and the Wannier function at lattice site j [59],

$$W_j(x,\varphi)=\sum_{0\leqslant k<1}e^{ikj}\Psi_k(x,\varphi), \tag{12}$$

where the Bloch wave function is

$$\Psi_k(x,\varphi)=\frac{1}{\sqrt{L}}\sum_{n=-\infty}^{\infty}\langle n|k,\varphi\rangle e^{-i(n+k)x}. \tag{13}$$

Here we choose a *smooth* gauge for the Bloch wave function, so the Wannier function is well localized [60].

Figure 2(d) shows the integrated current as a function of φ, calculated from Eq. (11) using a similar method to Ref. [61]. We see the function is "steplike": Flat regions correspond to slow transport, while the particle motion is rapid in the steep regions. This is further illustrated by the Wannier function in Fig. 2(c). During the slow transport, the Wannier function slowly drifts, while during the rapid transport, one peak drops in amplitude and a second peak rises. This corresponds to tunneling.

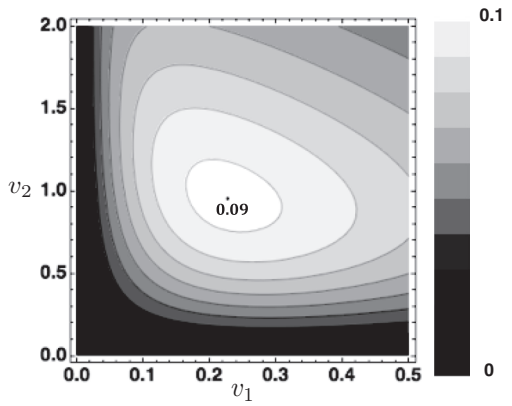

FIG. 3. Energy gap ΔE_g as a function of v_1,v_2 for $p=2,q=3$. The gap has a maximum value of $\Delta E_g\approx 0.09$ at $v_1=0.23$ and $v_2=0.95$.

For small v_1,v_2, the time scale for adiabaticity τ is related to the size of the gap, $1/\tau\sim|\alpha\Delta|\sim v_1^{|s_m|}v_2^{|r_m|}$. Thus when the Chern number $\mathcal{C}=s_m$ is large and the potentials are weak, adiabaticity is hard to maintain in a practical experiment. For large v_1,v_2, the gap again falls, owing to the large potential barriers. Figure 3 shows the energy gap ΔE_g as a function of v_1 and v_2 for $p=2,q=3$. The gap has a maximum value of $\Delta E_g\approx 0.09$ at $v_1=0.23$ and $v_2=0.95$. An optimized experiment would be performed with these parameters.

V. EXPERIMENTAL PROPOSAL

To observe this anomalous current, we envision a Fermi gas confined to a quasi-1D tube, such that only one transverse mode is occupied. Although the present analysis is 1D, we expect the phenomena will persist for more general transverse confinement. Along the tube, we engineer two longitudinal periodic potentials, $V_1(x,\varphi)=2v_1\cos(px-\varphi)$ and $V_2(x)=2v_2\cos(qx)$, via two pairs of counterpropagating laser beams. The time-dependent phase $\varphi=\delta\omega t$ is produced by a frequency difference $\delta\omega$ between two of the beams. To satisfy the adiabatic condition, we require $\hbar\delta\omega\ll\Delta E_g$. The resulting adiabatic particle current can be detected by observing the motion of the center of mass of the cloud: After time $t=2\pi N/\delta\omega$, the center of mass should move a distance $r_c=2\pi\mathcal{C}N/\kappa$. A dimensionless measure of this displacement is $x_c=\kappa r_c$. The displacement can be measured *in situ* [62–64] or after time of flight [65]. Similar experiments were proposed by Chiang and Niu [24] and Wang *et al.* [27].

We propose studying the case $p=2,q=3$, as this yields retrograde motion and has relatively large gaps (see Fig. 3).

In modeling this experiment, one must account for the finite cloud size. We include this physics by adding a harmonic potential along the tube, $V(x)=m\omega_0^2x^2/2$. Such potentials are always found in such experiments. Within a local density

approximation, the lowest band will be filled at the center of the cloud, but only partially filled near the edge. Although our Chern number argument only applies to the central region, we still expect the center-of-mass motion to be nearly quantized. For $\hbar\omega_0 \ll v_1, v_2$ and particle number much greater than one, only a very small portion of the particles live at boundaries. Our numerical simulations (detailed below) confirm this result. For a typical experiment, $\omega_0 \sim 10$ Hz and $v_1/\hbar, v_2/\hbar \sim 100$ kHz [67].

Because of the trap, the displacement r_c cannot be made arbitrarily large. When $m\omega_0^2 r_c^2/2$ is of the order of the band gap ΔE_g, atoms can tunnel to the higher bands. In our numerical simulation, we see that for small $\delta\omega$, the maximum displacement scales as $1/\omega_0$.

VI. NUMERICAL SIMULATION

In order to see the feasibility of our experimental proposal, we numerically simulate the dynamical evolution of a 1D Fermi gas. We take the many-body state to be a Slater determinant, made up from single-particle wave functions $\psi_i(x,t)$ with $1 \leqslant i \leqslant \nu$, where $\nu = 63$ is the number of fermions. This number is chosen because it is similar to typical atom numbers in 1D experiments [66]. At time $t = 0$, $\psi_i(x,0)$ is the ith eigenstate of the Hamiltonian. We evolve $\psi_i(x,t)$ via the time-dependent single-particle Schrödinger equation and then calculate the center of mass, $x_c(t) \equiv 1/\nu \sum_{i=1}^{\nu} \int x|\psi_i(x,t)|^2 dx$. Figure 4 shows the results for $p = 2, q = 3$ where the Chern number is $\mathcal{C} = -1$. We see $x_c < 0$, meaning that the particles travel in the *opposite* direction to the sliding potential. Remarkably this retrograde motion persists even for relatively large $\delta\omega$. As $\delta\omega \to 0$, the motion becomes quantized. A typical experiment has $E_r/\hbar \sim 100$ kHz [67], so the Chern number $\mathcal{C} = -1$ is readily extracted when $\delta\omega \lesssim 200$ Hz. The inset of Fig. 4 shows the evolution of the center of mass in one pumping cycle for $\hbar\delta\omega = 0.002E_r$. We see that the function is steplike, similar to the ideal case (no harmonic trap and adiabatic) in Fig. 2(d).

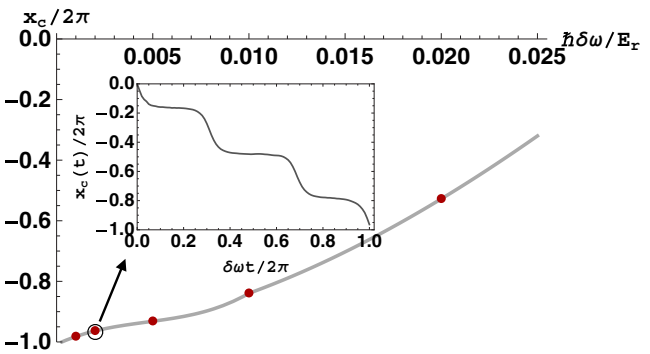

FIG. 4. (Color online) Displacement of the center of mass (in units of the superlattice) after one pumping period $T = 2\pi/\delta\omega$ for $\nu = 63$ fermions in a superlattice with $p = 2, q = 3, v_1 = 0.23E_r, v_2 = 0.95E_r$, and a harmonic trap $\hbar\omega_0 = 2.2 \times 10^{-3}E_r$. Physically, $\delta\omega$ is the detuning between the beams producing the lattice with wave number p. We see $x_c/2\pi \to C = -1$ as $\delta\omega$ decreases. Inset: The evolution of the center of mass for $\hbar\delta\omega = 0.002E_r$. Compare with Fig. 2(d).

VII. SUMMARY

To summarize, we studied topological charge pumping in a 1D sliding superlattice, with particular focus on the anomalous regimes where the particles move faster than the potential, or backwards. We presented a physical interpretation of this behavior in terms of the quantum tunneling of Wannier functions between minima in the potential. We proposed a practical cold-atom experiment to detect this phenomenon and calculated optimized parameters. Through numerical simulations, we confirmed that a *negative* integrated current and a nontrivial Chern number $\mathcal{C} = -1$ are readily measured.

ACKNOWLEDGMENTS

R.W. thanks Tomás Arias for useful discussions on computing the localized Wannier states. We acknowledge support from the ARO MURI Non-equilibrium Many-body Dynamics Grant No. W911NF-14-1-0003 and NSF PHY-1508300.

APPENDIX

Here we derive an effective Hamiltonian for Eqs. (4) and (5) in the main text. For small λ, the eigenstates of the lowest band will be superpositions of $|-1\rangle$ and $|0\rangle$, motivating projection operators

$$P = |-1\rangle\langle -1| + |0\rangle\langle 0|, \tag{A1}$$

$$Q = 1 - P. \tag{A2}$$

The states $|m\rangle = \psi_m^\dagger|\text{vac}\rangle$ satisfy $H_0|m\rangle = \frac{1}{2}(k_x + m)^2|m\rangle$. We seek eigenstates $H|\psi\rangle = E|\psi\rangle$. We break the wave function into two parts,

$$|\psi\rangle = P|\psi\rangle + Q|\psi\rangle \equiv |\psi_0\rangle + |\psi_{\text{ex}}\rangle, \tag{A3}$$

where $|\psi_0\rangle$ is in the low-energy sector and $|\psi_{\text{ex}}\rangle$ is a superposition of the higher-energy states. The eigenequation is then decoupled into two equations,

$$PH|\psi\rangle = PE|\psi\rangle = E|\psi_0\rangle, \tag{A4}$$

$$QH|\psi\rangle = QE|\psi\rangle = E|\psi_{\text{ex}}\rangle. \tag{A5}$$

Inserting the identity $P^2 + Q^2 = P + Q = 1$ on the left-hand side of Eqs. (A4) and (A5) and substituting $|\psi_{\text{ex}}\rangle$ in terms of $|\psi_0\rangle$, we obtain a closed equation for $|\psi_0\rangle$,

$$H_{\text{eff}}|\psi_0\rangle = E|\psi_0\rangle, \tag{A6}$$

where

$$H_{\text{eff}} \equiv PHP + PHQ\frac{1}{E - QHQ}QHP. \tag{A7}$$

Using the identity $PH_0Q = 0$ and expanding the second term of Eq. (A7), we obtain

$$H_{\text{eff}} = PH_0P + \lambda PH_1P + \lambda^2 PH_1Q\sum_{j=0}^{\infty}\frac{1}{E - QH_0Q} \times \left(\lambda\frac{QH_1Q}{E - QH_0Q}\right)^j QH_1P. \tag{A8}$$

This equation can be written as

$$H_{\text{eff}} = PH_0P + \sum_{\substack{s_+,s_- \geqslant 0 \\ r_+,r_- \geqslant 0}} \lambda_p^{s_+}\lambda_{-p}^{s_-}\lambda_q^{r_+}\lambda_{-q}^{r_-}\mathcal{L}^{(s_+,s_-,r_+,r_-)}, \quad \text{(A9)}$$

where the momentum conservation implies that $\alpha \equiv \langle -1|\mathcal{L}^{(s_+,s_-,r_+,r_-)}|0\rangle = 0$ unless $sp + rq = 1$, where $s = s_+ - s_-$ and $r = r_+ - r_-$. In our problem, the lowest-order contribution to α has either $s_+ = 0$ or $s_- = 0$. Similarly $r_+ = 0$ or $r_- = 0$. The lowest-order contribution to the diagonal elements of H_{eff} corresponds to an identity matrix.

Linearizing H_{eff} about $\delta k = 0$ and writing the operators in the basis $\{|-1\rangle, |0\rangle\}$, we have

$$\mathcal{H}_{\text{eff}} = \begin{pmatrix} -\frac{1}{2}\delta k & \alpha\Delta e^{i\chi} \\ \alpha\Delta e^{-i\chi} & \frac{1}{2}\delta k \end{pmatrix} + \text{const}, \quad \text{(A10)}$$

where $\Delta = v_1^{|r_m|}v_2^{|s_m|}$, $\chi = -s_m\varphi$, and s_m, r_m correspond to the absolutely smallest solution to the Diophantine equation $sp + rq = 1$.

[1] D. J. Thouless, Phys. Rev. B **27**, 6083 (1983).
[2] D. J. Thouless, M. Kohmoto, M. P. Nightingale, and M. den Nijs, Phys. Rev. Lett. **49**, 405 (1982).
[3] Q. Niu, Phys. Rev. B **34**, 5093 (1986).
[4] D. R. Hofstadter, Phys. Rev. B **14**, 2239 (1976).
[5] S. Aubry and G. André, Ann. Isr. Phys. Soc. **3**, 133 (1980).
[6] L.-J. Lang, X. Cai, and S. Chen, Phys. Rev. Lett. **108**, 220401 (2012).
[7] Z. Xu, L. Li, and S. Chen, Phys. Rev. Lett. **110**, 215301 (2013).
[8] Z. Xu and S. Chen, Phys. Rev. B **88**, 045110 (2013).
[9] L.-J. Lang and S. Chen, J. Phys. B: At. Mol. Opt. Phys. **47**, 065302 (2014).
[10] Y. E. Kraus, Y. Lahini, Z. Ringel, M. Verbin, and O. Zilberberg, Phys. Rev. Lett. **109**, 106402 (2012).
[11] Y. E. Kraus and O. Zilberberg, Phys. Rev. Lett. **109**, 116404 (2012).
[12] Y. E. Kraus, Z. Ringel, and O. Zilberberg, Phys. Rev. Lett. **111**, 226401 (2013).
[13] F. Grusdt, M. Höning, and M. Fleischhauer, Phys. Rev. Lett. **110**, 260405 (2013).
[14] S. Ganeshan, K. Sun, and S. Das Sarma, Phys. Rev. Lett. **110**, 180403 (2013).
[15] S.-L. Zhu, Z.-D. Wang, Y.-H. Chan, and L.-M. Duan, Phys. Rev. Lett. **110**, 075303 (2013).
[16] K. A. Madsen, E. J. Bergholtz, and P. W. Brouwer, Phys. Rev. B **88**, 125118 (2013).
[17] I. I. Satija and G. G. Naumis, Phys. Rev. B **88**, 054204 (2013).
[18] X. Deng and L. Santos, Phys. Rev. A **89**, 033632 (2014).
[19] F. Matsuda, M. Tezuka, and N. Kawakami, J. Phys. Soc. Jpn. **83**, 083707 (2014).
[20] D.-T. Tran, A. Dauphin, N. Goldman, and P. Gaspard, Phys. Rev. B **91**, 085125 (2015).
[21] F. Mei, S.-L. Zhu, Z.-M. Zhang, C. H. Oh, and N. Goldman, Phys. Rev. A **85**, 013638 (2012).
[22] P. Marra, R. Citro, and C. Ortix, Phys. Rev. B **91**, 125411 (2015).
[23] F. Liu, S. Ghosh, and Y. D. Chong, Phys. Rev. B **91**, 014108 (2015).
[24] Jing-Tzyh Alan Chiang and Q. Niu, Phys. Rev. A **57**, R2278 (1998).
[25] O. Romero-Isart and J. J. Garcia-Ripoll, Phys. Rev. A **76**, 052304 (2007).
[26] Y. Qian, M. Gong, and C. Zhang, Phys. Rev. A **84**, 013608 (2011).
[27] L. Wang, M. Troyer, and X. Dai, Phys. Rev. Lett. **111**, 026802 (2013).
[28] F. Mei, J.-B. You, D.-W. Zhang, X. C. Yang, R. Fazio, S.-L. Zhu, and L. C. Kwek, Phys. Rev. A **90**, 063638 (2014).
[29] D.-W. Zhang, F. Mei, Z.-Y. Xue, S.-L. Zhu, and Z. D. Wang, arXiv:1502.00059.
[30] P. G. Harper, Proc. Phys. Soc. Sec. A **68**, 874 (1955).
[31] M. Kohmoto, Ann. Phys. (Berlin) **160**, 343 (1985).
[32] M. Aidelsburger, M. Atala, S. Nascimbène, S. Trotzky, Y.-A. Chen, and I. Bloch, Phys. Rev. Lett. **107**, 255301 (2011).
[33] M. Aidelsburger, M. Atala, M. Lohse, J. T. Barreiro, B. Paredes, and I. Bloch, Phys. Rev. Lett. **111**, 185301 (2013).
[34] H. Miyake, G. A. Siviloglou, C. J. Kennedy, W. C. Burton, and W. Ketterle, Phys. Rev. Lett. **111**, 185302 (2013).
[35] M. Atala, M. Aidelsburger, M. Lohse, J. T. Barreiro, B. Paredes, and I. Bloch, Nat. Phys. **10**, 588 (2014).
[36] M. Aidelsburger, M. Lohse, C. Schweizer, M. Atala, J. T. Barreiro, S. Nascimbne, N. R. Cooper, I. Bloch, and N. Goldman, Nat. Phys. **11**, 162 (2015).
[37] A. Dauphin and N. Goldman, Phys. Rev. Lett. **111**, 135302 (2013).
[38] H. M. Price and N. R. Cooper, Phys. Rev. A **85**, 033620 (2012).
[39] X.-J. Liu, K. T. Law, T. K. Ng, and P. A. Lee, Phys. Rev. Lett. **111**, 120402 (2013).
[40] D. A. Abanin, T. Kitagawa, I. Bloch, and E. Demler, Phys. Rev. Lett. **110**, 165304 (2013).
[41] M. Atala, M. Aidelsburger, J. T. Barreiro, D. Abanin, T. Kitagawa, E. Demler, and I. Bloch, Nat. Phys. **9**, 795 (2013).
[42] F. Grusdt, D. Abanin, and E. Demler, Phys. Rev. A **89**, 043621 (2014).
[43] E. Alba, X. Fernandez-Gonzalvo, J. Mur-Petit, J. K. Pachos, and J. J. Garcia-Ripoll, Phys. Rev. Lett. **107**, 235301 (2011).
[44] E. Zhao, N. Bray-Ali, C. J. Williams, I. B. Spielman, and I. I. Satija, Phys. Rev. A **84**, 063629 (2011).
[45] D.-L. Deng, S.-T. Wang, and L.-M. Duan, Phys. Rev. A **90**, 041601(R) (2014).
[46] N. Goldman, J. Dalibard, A. Dauphina, F. Gerbierb, M. Lewensteine, P. Zoller, and I. B. Spielman, Proc. Natl. Acad. Sci. USA **110**, 6736 (2013).
[47] N. Goldman, J. Beugnon, and F. Gerbier, Phys. Rev. Lett. **108**, 255303 (2012).
[48] N. Goldman, J. Beugnon, and F. Gerbier, Europhys. J.: Spec. Top. **217**, 135 (2013).
[49] M. D. Reichl and E. J. Mueller, Phys. Rev. A **89**, 063628 (2014).
[50] B. K. Stuhl, H.-I. Lu, L. M. Aycock, D. Genkina, and I. B. Spielman, arXiv:1502.02496.

[51] M. Mancini, G. Pagano, G. Cappellini, L. Livi, M. Rider, J. Catani, C. Sias, P. Zoller, M. Inguscio, M. Dalmonte, and L. Fallani, arXiv:1502.02495.
[52] R. O. Umucalılar, H. Zhai, and M. Ö. Oktel, Phys. Rev. Lett. **100**, 070402 (2008).
[53] L. B. Shao, S.-L. Zhu, L. Sheng, D. Y. Xing, and Z. D. Wang, Phys. Rev. Lett. **101**, 246810 (2008).
[54] D. Xiao, M. Chang, and Q. Niu, Rev. Mod. Phys. **82**, 1959 (2010).
[55] M. Kohmoto, J. Phys. Soc. Jpn. **61**, 2645 (1992).
[56] D. Osadchy and J. E. Avron, J. Math. Phys. **42**, 5665 (2001).
[57] N. Goldman, J. Phys. B: At. Mol. Opt. Phys. **42**, 055302 (2009).
[58] J. E. Avron, O. Kenneth, and G. Yehoshua, J. Phys. A: Math. Theor. **47**, 185202 (2014).
[59] Q. Niu, Phys. Rev. Lett. **64**, 1812 (1990).
[60] N. Marzari, A. A. Mostofi, J. R. Yates, I. Souza, and D. Vanderbilt, Rev. Mod. Phys. **84**, 1419 (2012).
[61] T. Fukui, Y. Hatsugai and Hiroshi Suzuki, M. Kohmoto, J. Phys. Soc. Jpn. **74**, 1674 (2005).
[62] W. S. Bakr, A. Peng, M. E. Tai, R. Ma, J. Simon, J. I. Gillen, S. Fölling, L. Pollet, and M. Greiner, Science **329**, 547 (2010).
[63] N. Gemelke, X. Zhang, C.-L. Hung, and C. Chin, Nature (London) **460**, 995 (2009).
[64] J. F. Sherson, C. Weitenberg, M. Endres, M. Cheneau, I. Bloch, and S. Kuhr, Nature (London) **467**, 68 (2010).
[65] I. Bloch, J. Dalibard, and W. Zwerger, Rev. Mod. Phys. **80**, 885 (2008).
[66] Y. Liao, A. S. C. Rittner, T. Paprotta, W. Li, G. B. Partridge, R. G. Hulet, S. K. Baur, and E. J. Mueller, Nature (London) **467**, 567 (2010).
[67] M. Greiner, O. Mandel, T. Esslinger, T. W. Hänsch, and I. Bloch, Nature (London) **415**, 39 (2002).